Key Engineering Materials
ISSN: 1662-9795, Vol. 984, pp 9-15
doi:10.4028/p-9trMUe
© 2024 The Author(s). Published by Trans Tech Publications Ltd, Switzerland.
Submitted: 2023-10-01
Accepted: 2024-04-15
Online: 2024-08-22

Optical Ionization of Qubits and their Silent Charge States

Michel Bockstedte[1,a*], and Maximilian Schober[2,b]

Institute for Theoretical Physics, Johannes Kepler University Linz, Altenbergerstr. 69, A-4040 Linz, Austria

[a]Michel.Bockstedte@jku.at, [b]Maximilian.Schober@jku.at

Keywords: Silicon Vacancy, Photoionization Cross Section, *Ab Initio* Theory, Multiplet States

Abstract. Color centers in the technologically mature material silicon carbide are candidates for the implementation of quantum applications. Chargestate control and electrical read-out of qubits includes spin-to-charge conversion via optical excitation and subsequent ionization. In this work we address the dominant photoionization mechanism and the photophysical properties of the ionized silicon vacancy in 4H SiC using ab initio theory. We find that its nominally dark chargestates are infrared emitters.

Introduction

Prototypical color centers in silicon carbide implement quantum bit functionality via coupled electron spins and spin-dependent interactions including a spin-selective optical cycle. The latter also provides optical read-out of the spin state. Alternative routes are based on spin-selective ionization and electrical detection of photo currents that was demonstrated for NV-centers in diamond [1] and also in SiC for the silicon vacancy (V_{Si}) and di-vacancy ($V_C V_{Si}$) [2, 3]. The experiments were interpreted in terms a two-photon process that leads to the ionization of the color center into a silent charge state. A subsequent photo-assisted capture of a free carrier returns the color center to the active qubit charge state. While in the case of the di-vacancy the emission of a hole is involved in the first process [4, 5], electron emission was proposed for the silicon vacancy instead [2]. How the optical ionization yield and the spin contrast depend on the photon energy is an open question. Furthermore, little is known about the photophysics of the ionized color centers and the emission from the metastable low-spin states. Here we focus on the silicon vacancy and analyze the situation with ab initio theory capable of including the crucial multiplet physics of the ionized qubit centers[6]. We shine light onto ionizing single and two-photon processes relevant for optical charge state switching and electrical detection of the spin states. These processes convert the optically active negative silicon vacancy in to the neutral or doubly negative one, which do not emit photons in the visible range and thus are silent.

Theoretical Approach

The photo and spin physics of the silicon vacancy and di-vacancy color centers in SiC or the NV-center in diamond are dominated by correlated multiplet states [7, 8, 6, 10]. The color center is characterized by a high spin ground state and a first excited multiplet that constitute the principle optical transition. Spin-selective non-radiative recombination via intermediate low-spin multiplet states mediated by spin-spin or spin-orbit coupling features a spin contrast in the principle optical transitions of the different spin sublevels. A fully fledged treatment of the correlated multiplet states is out of the reach of standard density functional theory (DFT) and many-body perturbation theory in the GW and BSE approaches (e.g. [6]). Yet, DFT calculations provided important insight into the single particle electronic structure, ionization levels and vibrational properties, whenever states can be represented by single Slater determinants. In group theory analysis, however, the construction of fundamental multiplet states can be accomplished based on symmetry and insight in key defect levels within the band gap can be provided. This enables, for instance, analysis of the optical-spin-relaxation cycle or photoionization processes [11, 3] in a model-based approach together with parameters obtained from DFT. However, in some cases such as the silicon vacancy several fundamental doublet states were obtained [8, 9] that may interact with each other and form new states [12, 10]. In this case the group theory analysis falls short.

This article is an open access article under the terms and conditions of the Creative Commons Attribution (CC BY) license
(https://creativecommons.org/licenses/by/4.0)

Here we combine hybrid density functional theory and our CI-cRPA embedding approach [6]. The embedding CI-cRPA approach employs a configuration interaction (CI) hamiltonian and the screened Coulomb interaction as obtained within the constrained random phase approximation (cRPA). It is able to describe excited state of defects including complex multiplet excitations and their correlated spin-states [6, 10]. The CI-cRPA hamiltonian is constructed from DFT-derived Kohn-Sham basis states encompassing the localized defect states, extended band states, and defect resonances in the vicinity of the fundamental band edges of the spin-restricted electronic ground state of the defect obtained from hybrid-DFT calculations (see below). The CI basis is build from an initial reference ground state configuration, from which all other states are obtained via excitations. The excitation scheme includes all possible excitations between the localized defect orbitals as well as the largest defect resonance and single excitations from the extended states. We start the excitation scheme with all single excitations and subsequently extending this set of states by further excitation among the defect states. Double counting of the Coulomb interaction is corrected based on the mean-field Hartree-Fock scheme as outlined in [6].

In the framework of DFT as implemented in the VASP package [13], the color centers in 4H-SiC are described by large defect cell including 576 lattice sites. The wave functions are represented within the projector augmented wave method using a plane wave energy cut-off of 420 eV and an augmentation cut-off of 840 eV. The ground state is obtained by relaxing the configuration using a single k-point (Γ-point) until forces were smaller than 0.005 eV/Å. Charge state corrections for the calculation of ionization levels were included by employing scheme by Markov and Payne [14].

Ionization cross sections were calculated as described in the section on photoionization using two different schemes. The first scheme follows the ideas of Razinkovas et al. [11] based on the initial defect state and final charged defect state with an additional electron or hole in the extended manifold of states. The particle in the extended state is characterized by a k-vector inside the first Brillouin zone. The integration over the final states in k-space is done by using a dense $6 \times 6 \times 6$ Γ-centered k-point grid, which corresponds to $36 \times 36 \times 12$ grid in the primitive 4H-SiC unit cell. Due to the enormous numerical effort in such calculations, the PBE exchange-correlation functional instead of the more accurate but numerically unsustainable HSE06 functional is employed, as suggested earlier [11, 3]. Beyond the optical matrix elements and band dispersion energies, all other energy values are obtained via HSE06 or CI-cRPA calculations. As will be outlined below, this approach employs fixed orbitals of the reference charge state and as such misses orbital relaxation as well as additional correlation effects in the final state. The CI-cRPA approach allows for the inclusion of the latter. At present we, however, cannot perform extensive k-space sampling within this approach and have to restrict the available final states to the folded k-point set available in the supercell.

Electronic States of V_{Si}^{-} and the Silent Charge States V_{Si}^{0} and V_{Si}^{2-}

The electronic structure of the silicon vacancy essentially derives from the interaction of the four carbon dangling bonds adjacent to the vacant silicon site in the crystal field of 4H SiC with C_{3v} symmetry. In the single electron picture, this interaction results in three localized defect states $|v\rangle$, $|e_x\rangle$, and $|e_y\rangle$ (the latter are degenerate) within the fundamental band gap, as well as, a defect resonance $|u\rangle$ just below the valence band edge. In spin polarized hybrid DFT the energetic position of this resonance depends on the occupation of the defect states $|v\rangle$, $|e_x\rangle$, and $|e_y\rangle$. In case of the negatively charged silicon vacancy V_{Si}^{-} three electrons in the localized defect levels couple to a spin $3/2$ and lead to an exchange splitting of the u resonance with the opposite spin across the valence band edge. The excitation of an electron from this u-level to the localized defect levels comprise the two fundamental quartet excitations. The initial ground and the two excited states are the multiplet states ${}^4A_2$, ${}^4A_2'$, and ${}^4E$ with four magnetic sublevels with spin components $M = \pm 3/2$ and $\pm 1/2$ (cf. Tab. 1). Each of the quartets with $\pm 3/2$ is essentially described by one Slater determinant within CI-cRPA and are also accessible in (constrained) density functional theory, while the $\pm 1/2$ wave functions are composed of linear combinations of Slater determinants as predicted by group theory [8]. Due to the orbital degen-

Table 1: Multiplet states of the the silicon vacancy V_{Si}^{-} and its silent charge states V_{Si}^{0} and V_{Si}^{2-} as calculated with CI-cRPA. The energy positions are given in eV.

V_{Si}^{-} (h)				V_{Si}^{0} (h)				V_{Si}^{2-} (h)			
$^4A_2$	0.00	^2E	0.27	^1E	0.00	^3E	0.01	$^3A_2$	0.00	^1E	0.18
$^4A_2'$ (vert)	1.46	$^2A_2$	0.28				0.04	^3E	0.41	$^1A_1$	0.72
(ZPL)	1.34	$^2E'$	0.90	$^1A_1$	0.97	$^3A_2$	0.08			$^1E'$	0.81
^4E (vert)	1.52	$^2A_2$	1.30	$^1A_1'$	1.08	$^5A_2$	0.33				
(ZPL)	1.39	$^2E''$	1.31								
V_{Si}^{-} (c)				V_{Si}^{0} (c)				V_{Si}^{2-} (c)			
$^4A_2$	0.00	^2E	0.24	^1E	0.00	^3E	0.05	$^3A_2$	0.00	^1E	0.19
$^4A_2'$ (vert)	1.36	$^2A_2$	0.28				0.08	^3E	0.44	$^1A_1$	0.78
(ZPL)	1.25	$^2E'$	0.85	$^1A_1$	1.11	$^3A_2$	0.12			$^1E'$	0.89
^4E (vert)	1.47	$^2A_2$	1.10	$^1A_1'$	1.21	$^5A_2$	0.45				
(ZPL)	1.32	$^2E''$	1.11								

eracy of the ^4E quartet and strong electron-phonon coupling a dynamic Jahn-Teller effect occurs. This yields vibronic states with contributions from $^4A_2'$ and ^4E that explain the v1, v1' and v2 photo luminescence (PL) lines of V_{Si}^{-} at the hexagonal (V1, V1' lines) and the cubic (V2 line) lattice sites [15]. The PL-lines V1 and V2 used in experiment for photo current detected magneto resonance (PDMR) are essentially related to the transition between $^4A_2$ and $^4A_2'$. The low spin doublet states found in CI-cRPA are provided in Tab. 1 as well. They are not the focus here and are described in more detail in Refs. [10, 12].

Photoionization (PI) takes V_{Si}^{-} to either V_{Si}^{0} or V_{Si}^{2-} alongside electron or hole emission, respectively. In order to understand the available final states of PI we investigated the electronic structure of V_{Si} in these charge states. Relaxed ground state geometries were obtained within spin-polarized hybrid DFT. For V_{Si}^{0} two electrons remain in the localized defect states either occupying $|v\rangle$, $|e_x\rangle$ ($|v\rangle$, $|e_y\rangle$) or $|e_x\rangle$, $|e_y\rangle$. The former electron configuration yields a Jahn-Teller distorted ground state. The second configuration preserves C_{3v}-symmetry, however, requires a constrained DFT calculation, indicating that this electronic configuration is not the ground state one. Hence we use the distorted geometry. Regarding V_{Si}^{2-} in hybrid DFT, two electrons occupy $|v\rangle$ and two electrons couple in the e states to a high-spin configuration. The resulting relaxed geometry preserves C_{3v}-symmetry. The ground and excited multiplets obtained by CI-cRPA are shown in Tab. 1.

The ground state of V_{Si}^{0} is a ^1E singlet closely followed by a ^3E triplet. The Jahn-Teller distortion splits the degenerate ^3E level by ~ 40 meV, whereas the splitting in ^1E is negligible. Excited singlets $^1A_1$ and $^1A_1'$ occur just under the ionization threshold (see below). A $^3A_2$-triplet is found ~ 40 meV above the ^3E level and is the only other triplet state found below ionization threshold. Furthermore we encounter a quintet $^5A_2$. Other triplet and quintet states are found at and above the ionization threshold. The only internal excitations may take place in the singlet manifold with excitation energies ~ 1 eV. Note that the level positions provided in Tab. 1 refer to the ground state geometry. Relaxation of the defect upon excitation is not directly accessible in (constrained) DFT due to the correlated nature of the singlet states. This relaxation energy is expected in the range of 0.1-0.2 eV. The center nevertheless is an infrared emitter.

For V_{Si}^{2-}, we find a non-degenerate triplet ground state $^3A_2$ and degenerate ^3E triplet ~ 0.4 eV above the ground state. Among the singlets, we find a degenerate $^1E \sim 20$ meV above the ground state and subsequent levels $^1A_1$ and $^1E'$. With internal triplet and singlet transitions also this center is an infrared emitter.

Table 2: Ionization levels as obtained from hybrid-DFT in units of eV.

	V_{Si} (h)	V_{Si} (c)
$\varepsilon(0\|-)$	1.32	1.28
$\varepsilon(-\|2-)$	2.73	2.62

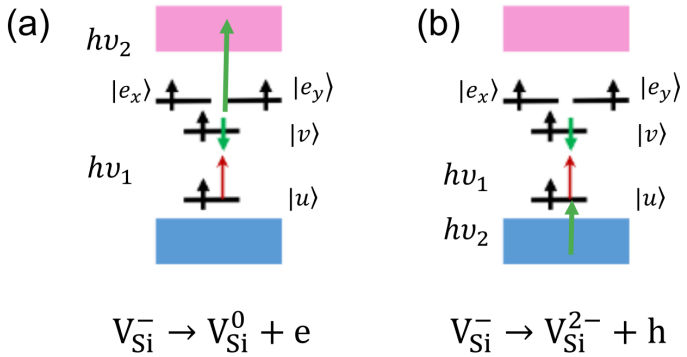

Fig. 1: Photoionization of V_{Si}^- via two subsequent photons $h\nu_1$ and $h\nu_2$ (a) to V_{Si}^0 with the emission of a defect electron into the conduction band, and (b) to V_{Si}^{2-} with excitation of a valence band electron into the defect states (hole emission). Note that the $|u\rangle$ level is drawn inside the band gap for easier readability, here the spin-up channel of this level actually forms a defect resonance (cf. text).

Two-Photon Photoionization of V_{Si}^-

Photoionization (PI) of V_{Si}^- on the one hand quenches the active charge state and its luminescence. This may be useful to switch off V_{Si}^--centers with detuned ZPLs. On the other hand, electric read-out contains spin-selective PI as a key step [2]. It should be noted, however, that the PI of other defect centers and the subsequent recombination of the emitted electrons or holes with V_{Si}^- will inevitably remove the active charge state [10] without being able to specifically address detuned V_{Si}^--centers. Hence the focus here is on the direct PI of the silicon vacancy. The PI by a single photon from the ground state requires photon energies $h\nu$ above a threshold energy ε_{thr} depending on the type of ionization process: (i) ionization of defect electron into the conduction band, i.e. $V_{Si}^- \rightarrow V_{Si}^0 + e$, with a threshold energy $\varepsilon_{\text{thr}}^h = \varepsilon(-|2-)$ or (ii) the excitation of a valence band electron into an unoccupied defect level alongside hole-emission, i.e. $V_{Si}^- \rightarrow V_{Si}^{2-} + h$, with a threshold energy $\varepsilon_{\text{thr}}^e = \varepsilon_{\text{gap}} - \varepsilon(0|-)$, where ε_{gap} is the fundamental band gap and $\varepsilon(0|-)$ and $\varepsilon(-|2-)$ are the ionization levels of V_{Si} with respect to the valence band edge. From the values listed in Tab. 2 it is clear that photon energies for resonant excitation of the V1 or V2 transition or those typically used in experiment (e.g. [10]) for excitation into their phonon side bands stay well below the single-photon ionization thresholds. Two-photon PI involves the ionization via an excited state by two subsequent photons, where the first one prepares the defect excited state and the second photon excites an electron from the valence band into the still excited defect or alternatively emits a defect electron into the conduction band. Such an ionization by the indicated two-photon processes is sketched in Fig. 1 and has recently been demonstrated [2] for V_{Si}^-. The energy of the first photon $h\nu_1$ must at least enable the resonant excitation of the V1 or V2 transitions or excite into the phonon sideband. The energy of the second photon $h\nu_2$ must exceed the minimum energy to enable ionization from the excited state. For the two processes indicated above, assuming resonant excitation with $h\nu_1$, the thresholds for $h\nu_2$ are given by $\varepsilon_{\text{thr,2PI}}^h = \varepsilon(-|2-) - E_{\text{ZPL}} + \Delta E_f^{\text{h}}$ and $\varepsilon_{\text{thr,2PI}}^e = \varepsilon_{\text{gap}} - \varepsilon(0|-) - E_{\text{ZPL}} + \Delta E_f^{\text{e}}$, respectively, where E_{ZPL} is the energy of the zero phonon line of the V1 or V2 excitation and ΔE_f^{h}, ΔE_f^{e} are the energy differences between the lowest allowed final

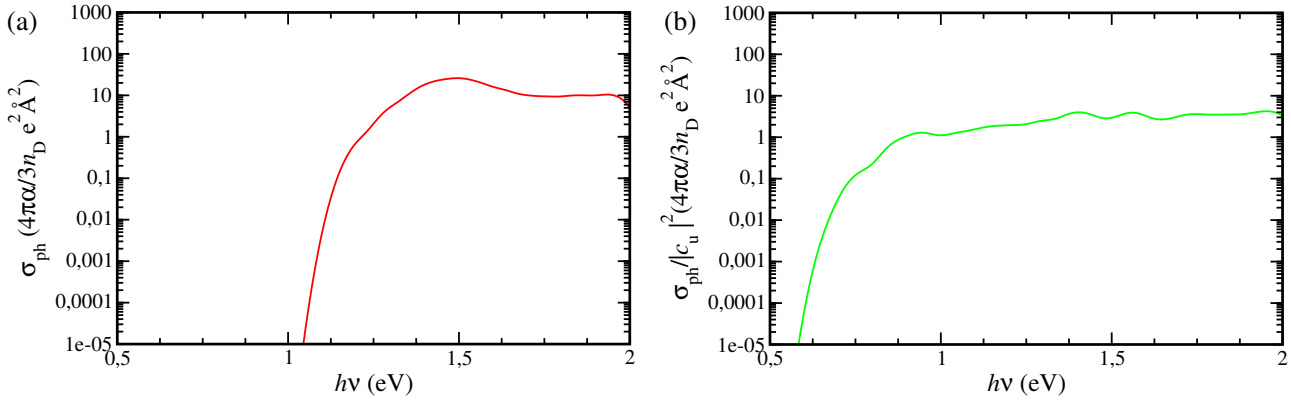

Fig. 2: Photoionization cross section (a) from ${}^4A_2$ to ${}^3A_2$ of V_{Si}^{2-} with the emission of a hole and (b) from ${}^4A_2$ to ${}^3E$ of V_{Si}^0 with the emission of an electron.

state of the ionized defect for ionization from the excited and ground state. Using the experimental value for the V1 (V2) lines we obtain the values listed in Tab. 2. Both thresholds are below the values for E_{ZPL}, hence a one color scheme with $h\nu_1 = h\nu_2$ is compatible with both ionization processes. The identification of the prevailing process, thus, cannot be accomplished simply by comparing threshold energies, instead the PI cross sections of the second excitation processes have to be compared. In the absence of lattice relaxation, it is given by [11]

$$\tilde{\sigma}_{\mathrm{PI}}(h\nu) = \frac{4\pi^2\,\alpha}{3\,n_D}\,h\nu \sum_{i,f} |\langle\Psi_i|\hat{\vec{D}}|\Psi_f\rangle|^2\,\delta(h\nu - (E_f - E_i)) \quad , \tag{1}$$

where α is the fine-structure constant, n_D is the refractive index of SiC, $\hat{\vec{D}}$ is the dipole operator, and $|\Psi_i\rangle$ ($|\Psi_f\rangle$) are the initial (final) states; the sum runs over all initial states, i.e. the degenerate sublevels of e.g. ${}^3E$ and all excited final states that derive from the (excited) ionized V_{Si} and an electron or hole in an extended state. Vibrational broadening is included in the cross section via the electron-phonon coupling $A(\varepsilon)$ (cf. Ref. [11] and references therein)

$$\sigma_{\mathrm{PI}}(\varepsilon) = \varepsilon \int_{\infty}^{\infty} \frac{1}{\varepsilon'}\,\tilde{\sigma}_{\mathrm{PI}}(\varepsilon)\,A(\varepsilon - \varepsilon')\,d\varepsilon' \quad . \tag{2}$$

In case of the NV-center [11], $\sigma_{\mathrm{PI}}(\varepsilon)$ is reduced by vibrational effects compared to $\tilde{\sigma}_{\mathrm{PI}}(\varepsilon)$ within the range of $\sim$1 eV above the ionization threshold. However, the values are within the same order of magnitude. From $\sim$ 1 eV towards higher energies $\sigma_{\mathrm{PI}}(\varepsilon)$ approaches $\tilde{\sigma}_{\mathrm{PI}}(\varepsilon)$. Similar effects are expected here for both ionized charge states of V_{Si}. For the purpose of the present paper, we therefore focus on $\tilde{\sigma}_{\mathrm{PI}}(\varepsilon)$ only.

As already mentioned in the theory section, two different approaches are employed for reasons outlined there. In the first one, we follow [11] and construct the final state $|\Psi_f\rangle$ from defect orbitals of V_{Si}^-. The initial state of V_{Si}^- of the two photon ionization is the ${}^4A_2'$. Its $M = \pm 3/2$ components are given in hole notation by $|ue_xe_y\rangle$ and $|\bar{u}\bar{e}_x\bar{e}_y\rangle$. Now, consider the ionization via excitation of the valence band electron into the empty u ($\bar{u}$) level. This directly produces $|he_xe_y\rangle$ ($|\bar{h}\bar{e}_x\bar{e}_y\rangle$), namely the ground state ${}^3A_2$ with an additional hole $|{}^3A_2, M = -1\rangle \otimes |h\rangle = |e_xe_y\rangle \otimes |h\rangle$ ($|{}^3A_2, M = 1\rangle \otimes |\bar{h}\rangle = |\bar{e}_x\bar{e}_y\rangle \otimes |\bar{h}\rangle$). The dipole matrix element $|\langle\Psi_i|\hat{\vec{D}}|\Psi_f\rangle|^2$ becomes the matrix element $|\langle h|\hat{\vec{D}}|v\rangle|^2$ of the corresponding Kohn-Sham orbitals. The same result is obtained for the initial state $|{}^4A_2, \pm 1/2\rangle$ except that here the excited state decomposes e.g. for $M = 1/2$ into $\sqrt{\frac{2}{3}}\,|{}^3A_2, 0\rangle \otimes |h\rangle$ and $\frac{1}{\sqrt{3}}\,|{}^3A_2, 1\rangle \otimes |\bar{h}\rangle$, both of which belong to the ground state of V_{Si}^{2-}. In Fig. 2(a) the resulting cross section is shown.

Furthermore, excitation to the ^3E excited state with an additional energy of $\sim 0.4\,\mathrm{eV}$ is possible, which only increases to the ionization cross section.

Next, we turn to the ionization via the excitation of a defect electron to the conduction band. Again, let the excitation starts from $|^4A_2', \pm 3/2\rangle$. The excitation e.g. for $M = -3/2$ directly produces $|ue_xe_y\bar{e}_y\rangle \otimes |c\rangle$, $|ue_x\bar{e}_xe_y\rangle \otimes |\bar{c}\rangle$, or $|uve_xe_y\rangle \otimes |c\rangle$ - where $|\bar{c}\rangle$ is an conduction band electron; the latter state is, however, higher in energy. After the detachment of the conduction band electron, this state indeed is an excited triplet state of $\mathrm{V}_{\mathrm{Si}}^0$ and is located at $\sim 1.6\,\mathrm{eV}$ above the ground state, well above the ionization threshold for hole emission. Therefore, from this state a quick recovery of $\mathrm{V}_{\mathrm{Si}}^-$ should take place. Furthermore, the corresponding matrix elements with the lowest stable triplet states ^3E (e.g. $|ve_xe_y\bar{e}_y\rangle \otimes |\bar{c}\rangle$) and $^3A_2$ (e.g. $|v\bar{v}e_xe_y\rangle \otimes |\bar{c}\rangle$) with the initial state vanishes exactly. This holds also true for the other stable states of $\mathrm{V}_{\mathrm{Si}}^0$. This would imply that no direct two-photon PI to $\mathrm{V}_{\mathrm{Si}}^0$ with electron emission should be possible. The shortcoming here is, however, that the orbitals $|u\rangle$, $|v\rangle$, $|e_x\rangle$, and $|e_y\rangle$ change their shapes in $\mathrm{V}_{\mathrm{Si}}^0$ compared to $\mathrm{V}_{\mathrm{Si}}^-$. This means that $|v\rangle$ should be replaced by $|v'\rangle$, which in the simplest approximation can be decomposed into $|v'\rangle = c_u\,|u\rangle + c_v\,|v\rangle$, where the complex coefficients c_u and c_v have to fulfill the normalization condition, such that $|c_u|^2 < 1$. Hybrid-DFT and CI-cRPA calculations suggest that $|c_u|^2 \sim 0.2$. Based on this argument, and by leaving $|e_x\rangle$ and $|e_y\rangle$ unchanged, we obtain dipole matrix elements $|c_u|^2\,|\langle x|\hat{\vec{D}}|c\rangle|^2$ and $|c_u|^2\,|\langle y|\hat{\vec{D}}|c\rangle|^2$ for the corresponding components of the ^3E triplet. The resulting cross section is proportional to $|c_u|^2$ and is shown modulo this value in Fig. 2b. A comparison of the two cross sections in Fig. 2 shows that the PI via $\mathrm{V}_{\mathrm{Si}}^{2-}$ alongside with hole emission is at least an order of magnitude larger than the process via $\mathrm{V}_{\mathrm{Si}}^0$ alongside with electron emission. Preliminary calculations of the full cross sections of the two mechanisms based on the CI-cRPA confirm this picture. There, we calculate the dipole matrix element directly for multiplet eigenstates of the CI hamiltonian with dominant single electron or hole excitations. These states already include charge relaxation in the excited state and some additional excitonic correlation. This leads to enhanced cross sections at specific energies for the PI via $\mathrm{V}_{\mathrm{Si}}^{2-}$, whereas for the other process we obtain maximal values than are one order of smaller than those shown in Fig. 2(b) indicating the effect of the coefficient $|c_u|^2$. However, as mentioned, in the method section, so far the sampling of conduction and valence band states is incomplete and we will provide numerical values at a later point.

Summary

In summary, we have investigated the photoionization of qubits in 4H-SiC and their silent charge states. With focus on the silicon vacancy, we use a theoretical approach capable of representing the correlated multiplet states. Our results indicate that the neutral and doubly negatively charged vacancies are infrared emitters albeit with optical transitions close to their ionization thresholds. The calculated photoionization cross sections show that the active qubit, the negatively charged silicon vacancy, is dominantly optically ionized to the doubly negatively charged defect alongside with emission of a hole. This rectifies an earlier assumption about the predominant mechanism in electrically detected magneto resonance.

Acknowledgement

The authors received financial support from the Austrian Science Fund (FWF, grant I5195) and German Research Foundation (DFG, QuCoLiMa, SFB/TRR 306, Project No. 429529648). The project profited from very generous computer time provided by the Erlangen National High Performance Computing Center (NHR@FAU) of the Friedrich-Alexander-Universität Erlangen-Nürnberg (FAU) and the Vienna Scientific Cluster (VSC).

References

[1] E. Bourgeois et al., Nat. Commun. **6**, 8577 (2015).

[2] Niethammer, et al., Nat. Commun. **10**, 5569 (2019).

[3] Ch. Anderson, et al., Science Adv. **8**, eabm5912 (2022)

[4] G. Wolfowicz, et al., Nat. Commun. **8**, 1876 (2018).

[5] Ch. Anderson, et al. Science **366**, 1225 (2019).

[6] M. Bockstedte, F. Schütz, Th. Garratt, V. Ivady, A. Gali, njp Quantum Materials **3**, 31 (2018).

[7] M. W. Doherty, et al., New J. Phys. **13**, 025019 (2011).

[8] Ö. O. Soykal, P. Dev, S. E. Economou, Phys. Rev. B **93**, 081207(R) (2016).

[9] W. Dong, M. W. Doherty, S. E. Economou, Phys. Rev. B **99**, 184102 (2019).

[10] M. Widmann, et al., Nano Lett. **19**, 7173 (2019).

[11] L. Razinkovas, et al., Phys. Rev. B **104**, 235301 (2021).

[12] M. Neubauer, M. Schober, W. Dobersberger, M. Bockstedte, conference proceedings of IC-SCRM 2023, submitted.

[13] G. Kresse, J. Furthmüller, Phys. Rev. B **54**, 11169 (1996). G. Kresse, D. Joubert, Phys. Rev. B **59**, 1758 (1999).

[14] G. Makov, M. C. Payne, Phys. Rev. B **51**, 4014 (1995).

[15] P. Udvarhely et al., Phys. Rev. Appl. **13**, 054017 (2020).